Solid State Science and Technology, Vol. 29, No 1 & 2 (2021) 22-31
ISSN 0128-7389 | *http://myjms.mohe.gov.my/index.php/masshp*

EFFECTS OF MICROSTRUCTURAL AND ORTHORHOMBICITY CHANGES ON THE SUPERCONDUCTING TRANSITION BEHAVIOR OF $YBa_2(Cu_{1-x}Zn_x)_3O_7$

Mabrouka Masoud[1], A. N. Jannah[2] and R. Abd-Shukor[1,*]

[1]*Department of Applied Physics, Universiti Kebangsaan Malaysia*
43600 Bangi, Selangor, Malaysia

[2]*Faculty of Applied Sciences, Universiti Teknologi MARA*
Negeri Sembilan Branch, Kuala Pilah Campus,
72000 Kuala Pilah, Negeri Sembilan, Malaysia

**Corresponding author: ras@ukm.edu.my*

Received: 24 November 2021
Accepted: 23 December 2021

ABSTRACT

The effects of Zn substitution on the superconducting transition behavior of $YBa_2(Cu_{1-x}Zn_x)_3O_{7-\delta}$ for x = 0 to 0.03 were investigated. The samples were prepared using the solid-state reaction method and characterized by using X-ray diffraction method (XRD), scanning electron microscope (SEM) and dc electrical resistance measurements. The XRD patterns showed that all samples consisted of the $YBa_2Cu_3O_{7-\delta}$ phase. The grain size did not change systematically with Zn substitution (~1.2 μm). However, the grain shape and boundaries were dramatically changed. The resistance (R) versus temperature (T) curves showed metallic normal state behavior for x = 0 and semiconductor-like behavior for all Zn substituted samples. The superconducting transition behavior was further investigated by plotting dR/dT versus T. The results showed that as Zn was substituted, two peaks were observed in the dR/dT curves where T_{p1} marks superconductivity within grains with the grain boundaries not yet superconducting and T_{p2} indicates the temperature where supercurrent flows between grains through proximity effects. All Zn substituted samples showed lowering of T_{p2} and broadening of DT_p (T_{p1} – T_{p2}). The changes in the grain shape, grain boundaries and orthorhombicity of the unit cell due to Zn substitution may have affected the superconducting transition behavior. The grains may have different T_cs due to orthorhombic-tetragonal transition and the samples became superconducting due to proximity effects between the inhomogeneous grains as the temperature was lowered to T_{p2}.

Keywords: electrical resistance; proximity effect; supercurrent

INTRODUCTION

The $YBa_2Cu_3O_{7-\delta}$ superconducts above liquid nitrogen temperature but this superconductor has some limitations for practical applications because of the low critical current density [1,3]. It is widely studied and the factors which suppress superconductivity continued to be explored. Elemental substitutions in the $YBa_2Cu_3O_{7-\delta}$ system continue to be of interest to researchers [1-13].

The effect of Zn on the properties of $YBa_2Cu_3O_{7-\delta}$ has been widely studied. XRD patterns indicate that the lattice parameters *a* and *b* of the samples increase slightly as the Zn concentration was increased because Zn^{2+} radius is slightly larger than Cu^{2+}. The orthorhombic–tetragonal (O-T) transition does show up in this system and this is due to Zn ions substitute mainly at the Cu(2) sites. The substitution leads to a change in oxygen stoichiometry and local lattice distortion. The Zn cation acts as a strong scattering center and induce local magnetic moment that increases with Zn concentration [4]. The normal and superconducting properties in $YBa_2(Cu_{1-x}M_x)_3O_7$ (M=Zn and Ni) have been investigated by ^{63}Cu NMR and NQR techniques. The non-magnetic Zn-doping into the CuO_2 plane in $YBa_2Cu_3O_7$ causes a local collapse of antiferromagnetic (AF) spin correlation near Zn impurities and induces a gapless superconductivity with a finite density of states at the Fermi surface [14].

The temperature versus oxygen content relevant to the doped elements suggests that different mechanisms drive the T_c reduction, depending on the site of substitution where electronic pair-breaking is dominant in CuO_2 substituted systems [15]. Changes of the field and temperature dependences of the magnetic susceptibility when Ba^{2+} is substituted with Sr^{2+} indicate an enhancement of the low-dimensional properties in the $DyBa_{2-x}Sr_xCu_3O_7$ system.[16]. The coexistence of magnetism and superconductivity was observed for $x \geq 0.3$ in the $Y_{1-x}Pr_xBa_2Cu_3O_{7-\delta}$ and magnetic ordering of Pr ions in this inhomogeneous system [17].

Although Zn substitution in $YBa_2Cu_3O_7$ have been reported, the combined effects of grain and grain boundary changes with the orthorhombic-tetragonal (O-T) transition on the superconducting transition behavior have not been well reported. The objective of this paper was to investigate the superconducting transition behavior of Zn substituted $YBa_2Cu_3O_7$ due to microstructural and orthorhombicity changes of the samples. We report results on phase, microstructure and transition behavior at T_c of Zn substituted $YBa_2(Cu_{1-x}Zn_x)_3O_{7-\delta}$. for x = 0 to 0.03.

MATERIALS AND METHODS

$YBa_2(Cu_{1-x}Zn_x)_3O_{7-\delta}$ (x = 0, 0.01, 0.02, 0.03) samples were prepared by the conventional solid-state reaction method using appropriate amounts of high purity (≥ 99.9%) powders of Y_2O_3, BaO, ZnO and CuO. The powders were mixed and ground in an agate mortar and pestle and calcined at 900 °C in alumina boats for 24 h and furnace cooled. After regrinding the material was recalcined at 900 °C for another 24 h. The

resultant powders were ground again and pressed into pellets of 12 mm diameter and 3 mm thickness. The pellets were heated in air at 900 °C for 24 h and cooled at around 1 °C/min.

The samples were analyzed with X-ray diffraction to determine the phase using a Siemen D-5000 diffractometer with CuK_α radiation from $2\theta = 2°$ to 60°. The lattice parameters were calculated by the least squares fitting method using at least 10 peaks using PTC Mathcad Prime 4.0 software. Scanning electron microscope (SEM) was used to observe the microstructure of the samples. In this work, a variable pressure scanning electron microscope (LEOVPSEM) was used. The average grain size was determined using the ImageJ software with at least 100 grains.

The superconducting transition temperature was determined by electrical resistance measurements using the four-probe technique. The experimental set-up consists of Keithley 220 Programmable Current Source, Keithley 197 Autoranging Microvolt DMM, Cryogenics 8200 Compressor, CTI-Cryogenics Model 22 Refrigerator, and Lakeshore 330 Auto-tuning Temperature controller. The distance between electrical contacts was about 1 mm and the current used was between 1 mA and 100 mA. Silver paste was used as electrical contacts.

RESULTS AND DISCUSSION

The X-ray diffraction patterns of $YBa_2(Cu_{1-x}Zn_x)_3O_{7-\delta}$ for x = 0.00, 0.01, 0.02 and 0.03 as illustrated in Figure 1 showed a dominant $YBa_2Cu_3O_7$ phase. Interestingly, the double-peaked features were visible for the (123) and (213) peaks pairs (at $2\theta \sim 60°$). The peaks pairs completely merge for x = 0.02 and x = 0.03. The calculated lattice parameters a, b and c versus Zn composition showed that all samples were single-phased with orthorhombic structure $a \neq b \neq c$ (Table 1). The orthorhombicity value ($e = (b-a)/(b+a)$) decreased with increase in Zn concentration for $YBa_2(Cu_{1-x}Zn_x)_3O_{7-\delta}$. This showed the occurrence of orthorhombic-tetragonal transition as Zn was substituted. The variation in lattice parameters can be attributed to the effect of slightly different ionic radius of Cu and Zn. The ionic radius with coordination number VI for Cu^{2+} is 0.73 Å, and Zn^{2+} is 0.74 Å. Hence, the slight increase in the unit cell volume was due to the slightly larger Zn^{2+} compared with Cu^{2+}.

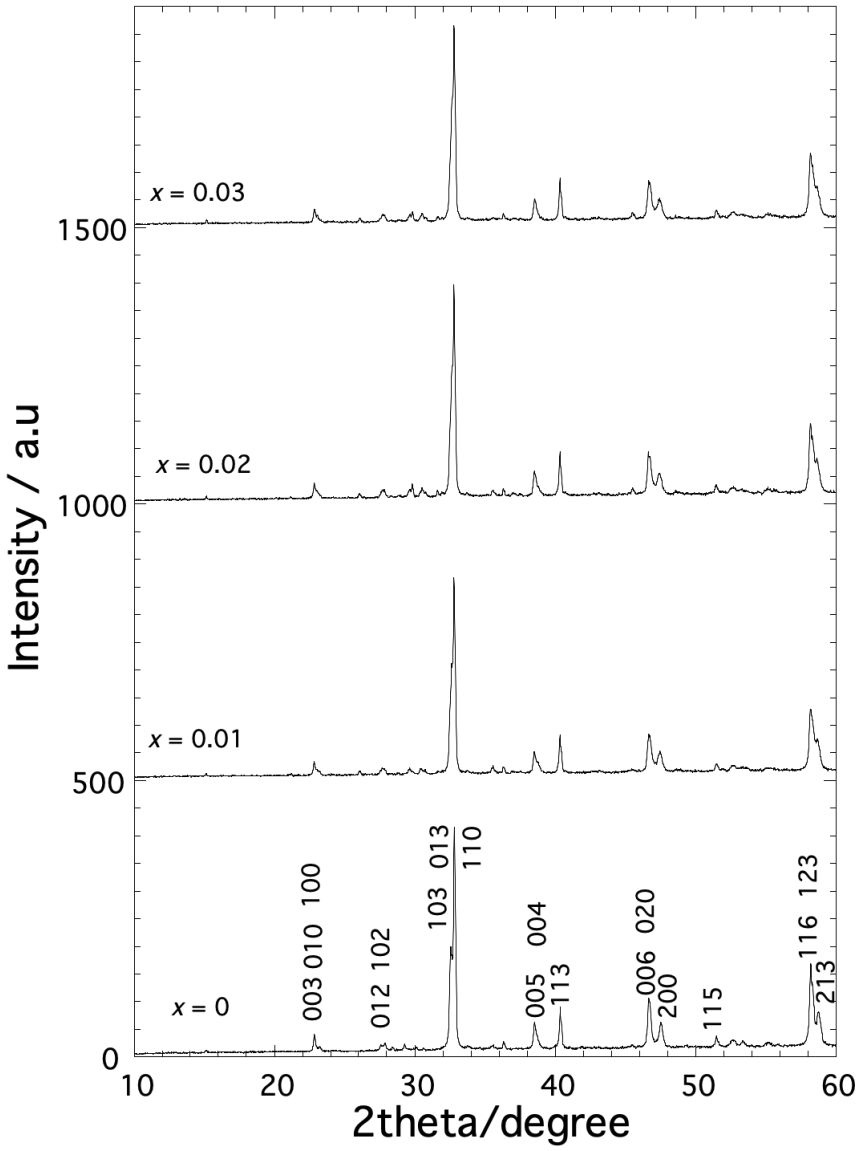

Figure 1: XRD patterns of $YBa_2(Cu_{1-x}Zn_x)_3O_{7-\delta}$ for x = 0, 0.01, 0.02 and 0.03

Table 1: $T_{c\ onset}$, $T_{c\ zero}$, ΔT_c, T_{p1}, T_{p2}, ΔT_p, lattice parameter *a, b, c*, unit cell volume and orthorhombicity of $YBa_2(Cu_{1-x}Zn_x)_3O_{7-\delta}$

x	0	0.01	0.02	0.03
a / Å	3.824	3.831	3.831	3.834
b / Å	3.878	3.873	3.873	3.874
c / Å	11.678	11.674	11.673	11.672
V / Å^3	173.18	173.21	173.20	173.36
e	0.00701	0.00545	0.00545	0.00519
$T_{c\text{-}onset}$ / K	95	69	58	53
$T_{c\text{-}zero}$ / K	88	44	28	26
ΔT_c / K	7	25	30	27
T_{p1}	90	60	46	41
T_{p2}	90	51	42	33
ΔT_p / K	0	9	4	8

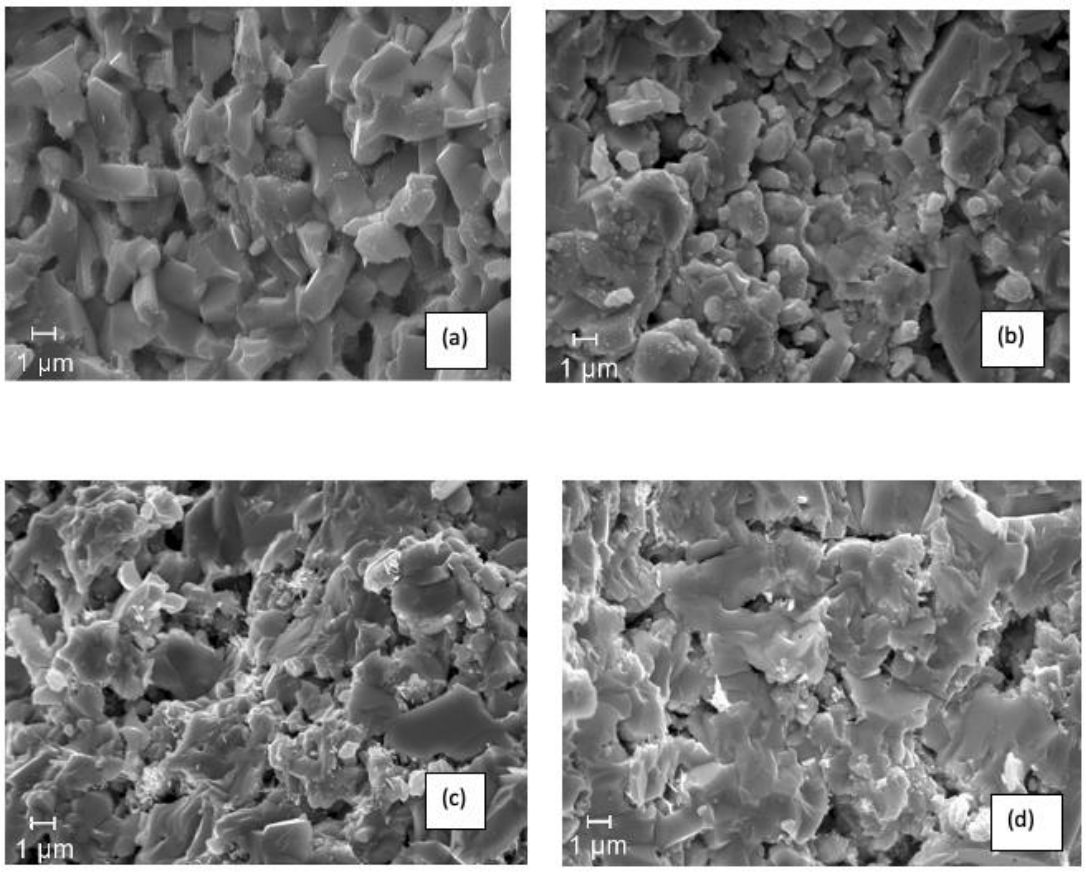

Figure 2: Scanning electron micrographs of $YBa_2(Cu_{1-x}Zn_x)_3O_{7-\delta}$ for (a) x = 0, (b) x = 0.01, (c) x = 0.02 and (d) x = 0.03

The SEM showed granular structures which is a characteristic of $YBa_2Cu_3O_7$ superconductor (Figure 2). Most of the samples showed a dense microstructure with

low porosity. The grain size histograms for all samples are shown in Figure 3. The average grain size of $YBa_2Cu_3O_7$ is ~ 1.2 μm and some gaps and voids were also observed. There was a slight change in grain shape when Zn was substituted which affected the nature of the grain boundaries. The x = 0 sample showed a fairly well-defined grain boundary. However, when Zn was substituted the grain boundaries were not well defined especially for the x = 0.02 and 0.03 samples most probably due to partial melting of the samples.

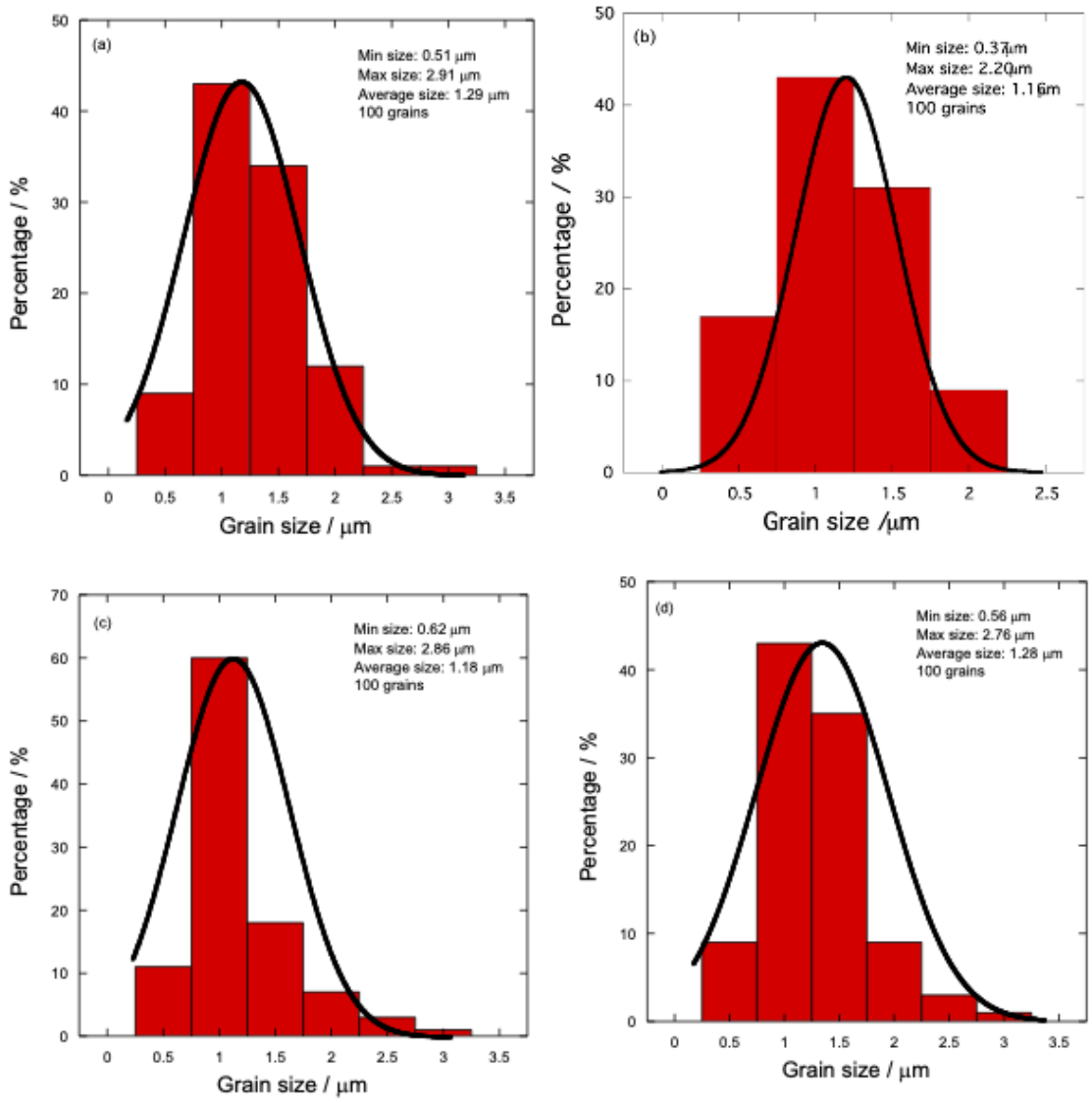

Figure 3: Histogram of grain size distribution of $YBa_2(Cu_{1-x}Zn_x)_3O_{7-\delta}$ for (a) x = 0, (b) x = 0.01, (c) x = 0.02 and (d) x = 0.03

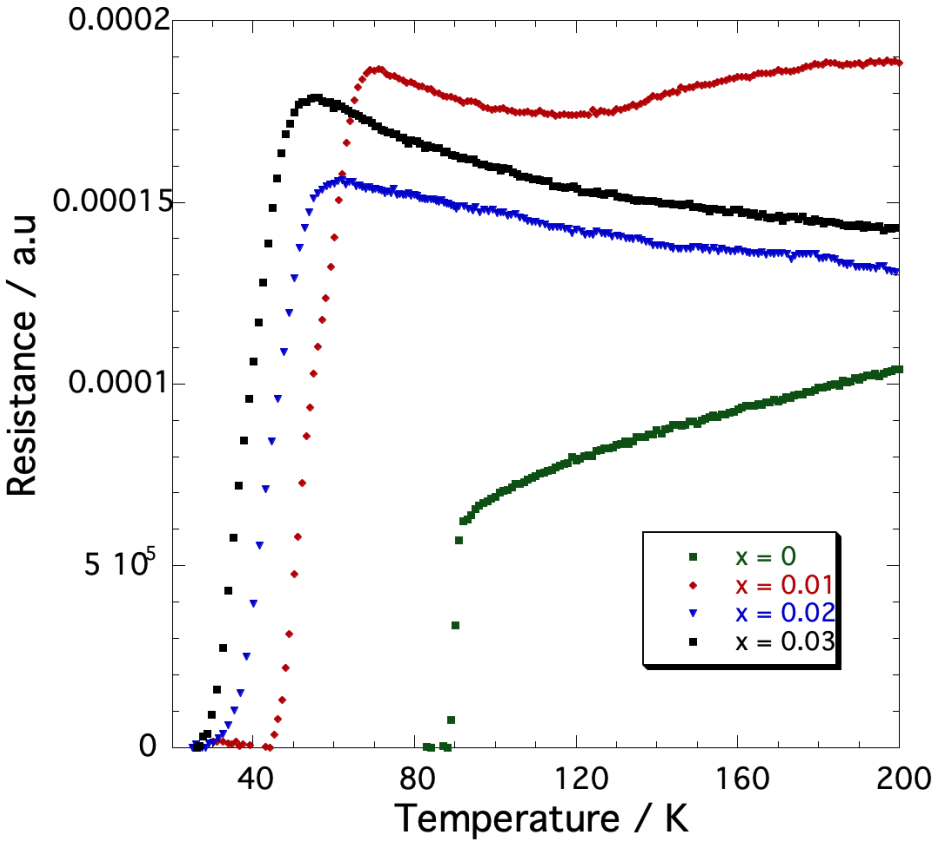

Figure 4: $T_{c\text{-onset}}$ and $T_{c\text{-zero}}$ versus Zn content of $YBa_2(Cu_{1-x}Zn_x)_3O_{7-\delta}$ for x = 0 - 0.03

The resistance-temperature curves for $YBa_2(Cu_{1-x}Zn_x)_3O_{7-\delta}$ are shown in Figure 4. The non-substituted sample showed metallic normal-state behavior. All Zn substituted samples for $YBa_2(Cu_{1-x}Zn_x)_3O_{7-\delta}$ exhibited semiconducting behavior persisting with Zn doping. This can be explained as a disorder due to the random distribution of inhomogeneities inside $YBa_2(Cu_{1-x}Zn_x)_3O_{7-\delta}$. The onset superconducting transition temperature, $T_{c\text{-onset}}$ were 95 K, 69 K, 58 K and 53 K for x = 0, 0.01, 0.02 and 0.03 respectively. The transition width DT_c increased with increasing Zn content. This decrease of the transition temperature is in agreement with previous reports [4, 9]. The suppression of T_c can be attributed to two possible mechanisms. This can be due to the Zn ion acting as a strong in-plane scattering center and also in part due to the loss in oxygen content as Zn was substituted for Cu. Zn substituted for Cu occupied the Cu planar site. This substitution leads to a change in oxygen content and local lattice distortion. Zn doping gives rise to redistribution of charge that produces strong electron scattering which breaks the coupling between Cooper pairs, therefore decreases T_c rapidly. $T_{c\text{-onset}}$, zero resistance temperature, $T_{c\text{-zero}}$, and ΔT_c are shown in Table 1 and Figure 5. $T_{c\text{-onset}}$ and $T_{c\text{-zero}}$ for $YBa_2(Cu_{1-x}Zn_x)_3O_{7-\delta}$ were severely suppressed with increasing Zn for $x \geq 0.01$. The superconducting transition width increased with increasing Zn content.

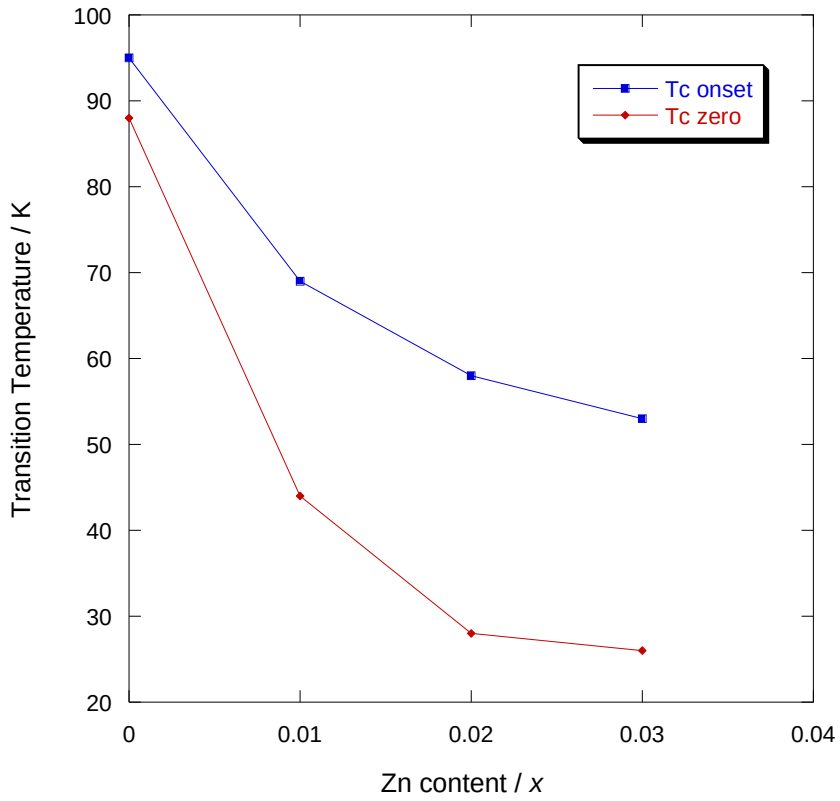

Figure 5: Transition temperature versus temperature of $YBa_2(Cu_{1-x}Zn_x)_3O_{7-\delta}$ for x = 0 - 0.03

To investigate this transition behavior further, the derivative of resistance with respect to temperature (dR/dT) curves were plotted (Figure 6). Two peaks were observed where T_{p1} marks superconductivity within grains but the grain boundaries are not yet superconducting [18]. T_{p2} indicates the temperature where supercurrent flows between grains through proximity effects. The transition width between the peaks DT_p (T_{p1} − T_{p2}) of the x = 0 samples was 0 K. This means that the superconductivity inside the grain and between grains occurred at about the same temperature. However, when Zn was substituted DT_p widened to between 4 and 9 K. The lowering of T_{p2} and broadening of DT_p reflects the effect of Zn substitution where small impurity phase may have resided at the grain boundaries and the whole sample becomes superconducting only when the temperature was lowered to T_{p2} due to proximity effect. Another explanation is the O-T transition which occurred as Zn was substituted. This can result in the inhomogeneous oxygen content of the unit cells and also the superconducting grain. Each grain may have different range of T_c from low to high temperature which can result in the widening of DT_p and DT_c. Table 1 shows $T_{c\text{-onset}}$, $T_{c\text{-zero}}$, ΔT_c, T_{p1}, T_{p2} and ΔT_p of $YBa_2(Cu_{1-x}Zn_x)_3O_{7-\delta}$.

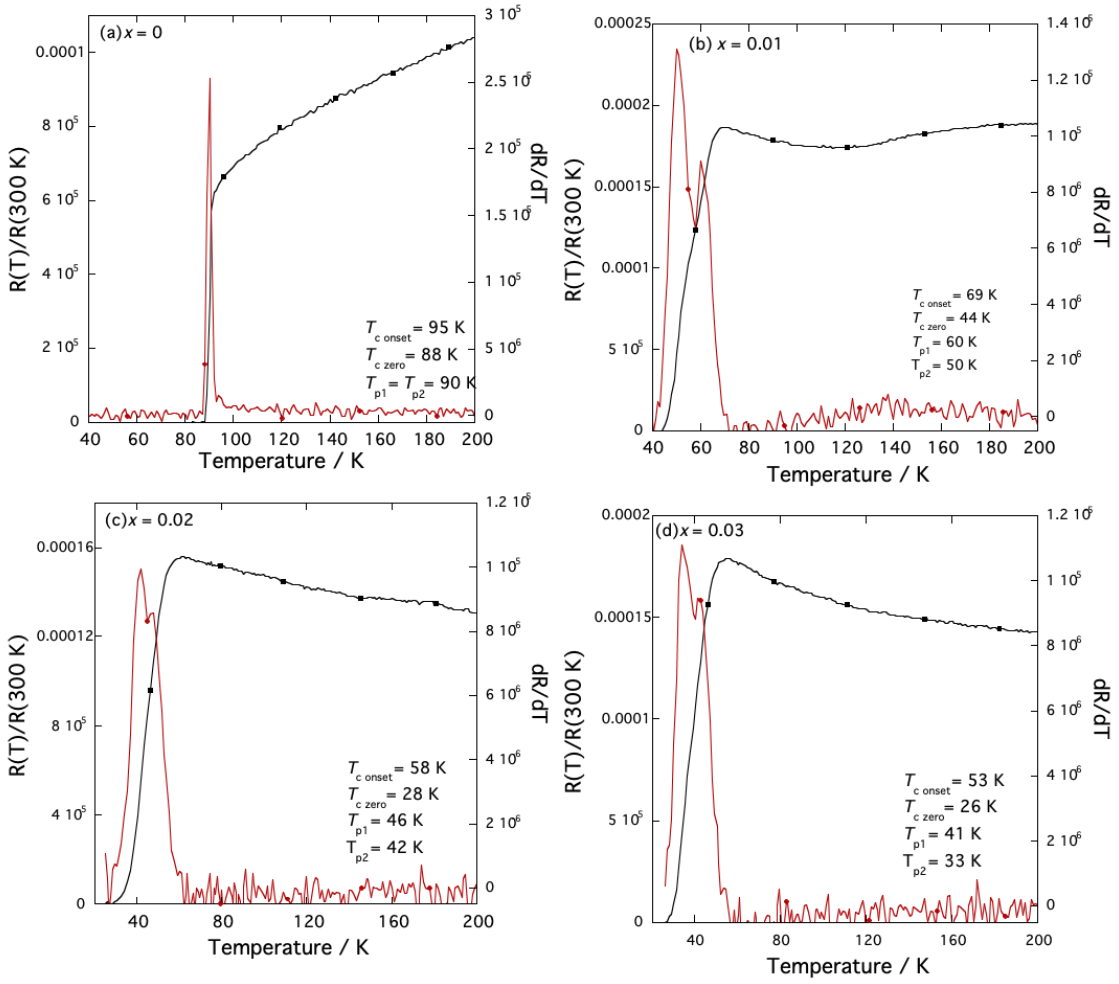

Figure 6:Electrical resistance and dR/dT versus temperature of $YBa_2(Cu_{1-x}Zn_x)_3O_{7-\delta}$ for x = 0 - 0.03

CONCLUSIONS

The effects of Zn substitution on $YBa_2(Cu_{3-x}Zn_x)O_{7-\delta}$ with x = 0 – 0.03 were studied. The zero-resistance temperature $T_{c\text{-zero}}$ decreased abruptly with Zn substitution consistent with O-T transition. This also indicated weakened inter-granular coupling due to changes at the grain boundaries as Zn was substituted. Other factors that contributed to this suppression may also be the inhomogeneous transition temperature of the individual grains as Zn content was increased. Further works on the relation between grain boundaries and O-T transition of other metal substituted (M) $YBa_2(Cu_{1-x}M_x)_3O_{7-\delta}$ is needed to confirm this assertion.

ACKNOWLEDGEMENTS

This work was supported by the Ministry of Higher Education, Malaysia under grant number FRGS/1/2020/STG07/UKM/01/1. A. N. Jannah thanks Universiti Teknologi Mara, Malaysia and Ministry of Higher Education, Malaysia for the post-doctoral grant.

REFERENCES

[1] Van Tendeloo, G., Krekels, T., Milat, O. and Amelinckx, S. *J. Alloys Compd.* **195** 307-314 (1993)
[2] Zhetpisbaev, K., Kumekov, S., Suib, N. R. M., Bakar, I. P. A. and Abd-Shukor, R. *Int. J. Electrochem. Sci*. **14**, 279-286 (2019)
[3] Ping-Lin, L., Yong-Yong, W., Yong-Tao, T., Jing, W., Xiao-Li, N., Jun-Xi, W., Dan-Dan, W. and Xiao-Xia, W. *Chinese Physics B* **17(9)** 3484 (2008)
[4] Singhal, R. K. *J. Alloys Compd.* **495(1)** 1-6 (2010)
[5] Singhal, R. K. *Materials Letters* **65(5)** 825-827 (2011)
[6] Slimani, Y., Almessiere, M. A., Hannachi, E., Mumtaz, M., Manikandan, A., Baykal, A. and Azzouz, F. B. *Ceramics International* **45(6)** 6828-6835 (2019)
[7] Vieira, V. N., Pureur, P. and Schaf, J. *Physica C: Supercond.* **353(3-4)** 241-250 (2001)
[8] Yahya, A. K., Yusof, M. I., Musa, B., Abdullah, W. F., Zamri, Z. and Jumali, M. H. *J. Appl Sci* **8(6)** 1007-1013 (2008)
[9] Zhang, L., Yu, L. P., Zhang, W., Wang, Y. Z., Zhang, H. and Zhao, Y. *Physica C: Supercond.* **357** 194-196 (2001)
[10] Al-Sharabi, A. N. N. A. S., Tajuddin, S. Y., Saffiey, A. D. F. W. and Jasman, S. *Sains Malaysiana* **45(12)** 1959-1969 (2016)
[11] Aminov, L. K., Ivanshin, V. A., Kurkin, I. N., Gafurov, M. R., Salikhov, I. K., Keller, H. and Gutmann, M. *Physica C: Supercond.* **349(1-2)** 30-34 (2001)
[12] Arif, M., Rahim, M. and Khan, N. A. *Ceramics International* **46(3)** 3218-3223 (2020)
[13] Furuyama, M., Iguchi, I., Kobayashi, N. and Muto, Y. *Physica B: Condens. Matter* **165** 1191-1192 (1990)
[14] Ishida, K., Kitaoka, Y., Ogata, N., Kamino, T., Asayama, K., Cooper, J. R. and Athanassopoulou, N. *J. Phys. Soc. Japan* **62(8)** 2803-2818 (1993)
[15] Licci, F. and Raffo, L. *Supercond Sci and Technol.* **8(4)** 245 (1995)
[16] Dyakonov, V. P., Markovich, V. I., Puzniak, R., Szymczak, H., Doroshenko, N. A. and Yuzhelevskii, Y. I. *Physica C: Supercond.* **225(1-2)** 51-58 (1994)
[17] Pradhan, A. K., Roy, S. B., Chaddah, P., Chen, C. and Wanklyn, B. M. *Physica C: Supercond.* **245(3-4)** 238-244 (1995)
[18] Sahoo, M. and Behera, D. *J. Phys. Chem. of Sol.* **74** 950-958 (2013)